HHS Public Access

Author manuscript

Respir Physiol Neurobiol. Author manuscript; available in PMC 2017 April 01.

Published in final edited form as:

Respir Physiol Neurobiol. 2016 April ; 224: 52–61. doi:10.1016/j.resp.2014.11.004.

Respiratory neuron characterization reveals intrinsic bursting properties in isolated adult turtle brainstems (*Trachemys scripta*)

Stephen M. Johnson[1], **Michael S. Hedrick**[2], **Bryan M. Krause**[3], **Jacob P. Nilles**[1], and **Mark A. Chapman**[1]

[1]Department of Comparative Biosciences, School of Veterinary Medicine, University of Wisconsin, Madison, Wisconsin 53706

[2]Department of Biological Sciences, California State University, East Bay, Hayward, CA 94542

[3]Neuroscience Training Program, University of Wisconsin, Madison, Wisconsin 53706

Abstract

It is not known whether respiratory neurons with intrinsic bursting properties exist within ectothermic vertebrate respiratory control systems. Thus, isolated adult turtle brainstems spontaneously producing respiratory motor output were used to identify and classify respiratory neurons based on their firing pattern relative to hypoglossal (XII) nerve activity. Most respiratory neurons (183/212) had peak activity during the expiratory phase, while inspiratory, post-inspiratory, and novel pre-expiratory neurons were less common. During synaptic blockade conditions, ~10% of respiratory neurons fired bursts of action potentials, with post-inspiratory cells (6/9) having the highest percentage of intrinsic burst properties. Most intrinsically bursting respiratory neurons were clustered at the level of the vagus (X) nerve root. Synaptic inhibition blockade caused seizure-like activity throughout the turtle brainstem, which shows that the turtle respiratory control system is not transformed into a network driven by intrinsically bursting respiratory neurons. We hypothesize that intrinsically bursting respiratory neurons are evolutionarily conserved and represent a potential rhythmogenic mechanism contributing to respiration in adult turtles.

1. Introduction

Neurons with intrinsic bursting properties spontaneously fire bursts of action potentials in the absence of synaptic inputs. Early analysis of invertebrate neural networks suggested that intrinsically bursting neurons were abundant in networks that continuously produced rhythmic motor behavior (Getting, 1988). Since breathing is a motor behavior that is

Corresponding Author: Stephen M. Johnson, M.D., Ph.D., Associate Professor, Department of Comparative Biosciences, School of Veterinary Medicine, University of Wisconsin, 2015 Linden Drive, Madison, Wisconsin 53706, Phone: (608) 263-39260, Fax: (608) 263-3926, johnsons@svm.vetmed.wisc.edu.

required from birth to death, a subpopulation of interconnected respiratory intrinsically bursting neurons was postulated to contribute to respiratory rhythm generation (Feldman and Cleland, 1982). Consistent with this hypothesis, intrinsically bursting respiratory neurons are found in perinatal rodent *in vitro* preparations that produce respiratory-related motor output, especially in the pre-Bötzinger Complex (preBötC) (Smith et al., 1991; Johnson et al., 1994; Rekling and Feldman, 1998; Thoby-Brisson and Ramirez, 2000, 2001; Pena et al., 2004) and para-Facial Respiratory Group (pFRG; Onimaru et al., 1989, 1995, 2003). The preBötC and the pFRG are coupled oscillatory networks that are hypothesized to be the sites of inspiratory and expiratory rhythm generation (Feldman and Del Negro, 2006; Feldman et al., 2013). The hybrid pacemaker-network model proposed that intrinsically bursting neurons played a critical role in respiratory rhythm generation (Funk and Feldman, 1995; Ramirez et al., 1997; Butera et al., 1999a, b; Koshiya and Smith, 1999; Smith et al., 2000; Peña et al., 2004). This hypothesis, however, is criticized because rhythmic activity persists when specific ion currents underlying intrinsic bursting activity are blocked (Del Negro et al., 2005). Instead, respiratory rhythm generation is hypothesized to require excitatory synaptic transmission in the dendrites to activate inward currents to produce the large depolarizing burst in respiratory neurons ("group pacemaker" model; Rekling and Feldman, 1998; Del Negro et al., 2002; Feldman and Del Negro, 2006; Mironov, 2008; Rubin et al., 2009; Del Negro et al., 2010; Feldman et al., 2013).

Intrinsically bursting respiratory neurons are hypothesized to be expressed primarily in young mammals, and sparsely expressed in adult mammals as synaptic inhibition increases and becomes the dominant mechanism for rhythm generation (Richter and Spyer, 2001; Broch et al., 2002; Richter and Smith, 2014). However, this hypothesis has not been tested in fully mature mammals, and it is not known whether intrinsically bursting neurons are expressed or contribute to respiratory rhythm generation in fully mature rodents, other mammals, or in non-mammalian vertebrates, in part due to significant technical difficulties in the experimental approach. At best, intrinsically bursting respiratory neurons are found in the preBötC of older perfused juvenile rat (P14-P21) and mouse (P21-P42) preparations (Paton, 1997; St. John et al., 2009). Second, most studies examining intrinsically bursting respiratory neurons focused on the preBötC and pFRG regions and did not test neurons in other brainstem regions. Third, no studies have tested for intrinsically bursting respiratory neurons in ectothermic vertebrates and thereby added a comparative and evolutionary perspective to this debate.

For ectothermic vertebrates, the potential existence of intrinsically bursting respiratory neurons was suggested by showing that rhythmic activity persists during synaptic inhibition blockade in isolated brainstems from tadpoles (Galante et al., 1996; Broch et al., 2002), adult lampreys (Rovainen, 1983), and adult turtles (Johnson et al., 2002). With synaptic inhibition blocked or severely attenuated, the persistent rhythm is thought to be due to intrinsically bursting respiratory neurons that continue to generate a wave of excitatory synaptic drive through the respiratory network to the respiratory motoneurons. Although this is the working hypothesis, experimental evidence directly demonstrating this principle is lacking. Finally, no studies have tested whether respiratory neurons in ectothermic vertebrates have intrinsic bursting properties.

To address these questions, brainstems from adult red-eared slider turtles were isolated under *in vitro* conditions and silicon multichannel electrodes were used to identify respiratory neurons and test for intrinsic bursting properties. Isolated turtle brainstems are advantageous because they produce expiratory- and inspiratory-related motor output that is qualitatively similar to that produced by intact turtles (Johnson and Mitchell, 1998). Also, since this turtle species is extremely resistant to hypoxia (Jackson, 2000; Johnson et al., 1998), respiratory motor output can be produced on the XII nerve root of isolated turtle brainstems for several days at physiologically relevant temperatures (Wilkerson et al., 2003). Our goals were to: (1) identify respiratory neurons in the turtle brainstem and expand on the initial map generated by Takeda et al. (1986); (2) classify respiratory neurons based on their firing pattern relative to the XII motor discharge; (3) test whether respiratory neurons express intrinsic bursting properties by blocking synaptic transmission (via a cocktail of drugs that block excitatory and inhibitory synaptic transmission); (4) determine whether intrinsic bursting respiratory neurons belong to a specific type or are localized within specific brainstem region; and (5) test whether synaptic inhibition blockade transforms the firing pattern of respiratory neurons or results in non-specific seizure-like activity. Preliminary reports of this work were published in abstract form (Chapman and Johnson, 2008).

2. Methods

All procedures were approved by the Animal Care and Use Committee at the University of Wisconsin-Madison School of Veterinary Medicine. Adult red-eared slider turtles (*Trachemys scripta*, n = 21, 689 ± 200 g) were obtained from commercial suppliers and kept in a large open tank where they had access to water for swimming and heat lamps and dry areas for basking. Room temperature was set to 27–28°C with light provided 14 h/day. Turtles were fed ReptoMin® floating food sticks (Tetra, Blackburg, VA, USA) 3–4 times per week.

2.1 Turtle brainstem preparations

Turtles were intubated and anesthetized with 5% isoflurane (balance oxygen) until the head and limb withdrawal reflexes were eliminated, after which the turtles were decapitated. The brainstem was removed and pinned onto Sylgard® in a recording chamber. The tissue was superfused with artificial cerebrospinal fluid (“aCSF solution”) containing HEPES (N-[2-hydroxyethyl]piperazine-N′-[2-ethane-sulfonic acid]) buffer as follows (mM): 100 NaCl, 23 $NaCHO_3$, 10 glucose, 5 HEPES (sodium salt), 5 HEPES (free acid), 2.5 $CaCl_2$, 2.5 $MgCl_2$, 1.0 K_2PO_4, and 1.0 KCl. The HEPES solution was bubbled with 5% CO_2-95 % O_2 (pH = ~7.35).

2.2 Cranial nerve recordings

Glass suction electrodes were attached to XII nerve rootlets. Signals were amplified (10,000x) and band-pass filtered (1–500 Hz) using a differential AC amplifier (model 1700, A-M Systems, Everett, WA, USA) before being rectified and integrated (time constant = 200 ms) using a moving averager (MA-281/RSP, CWE, Inc., Ardmore, PA, USA) (see Figs.

1A, 1C). The signals were digitized (RP2.1, Tucker-Davis Technologies, Alachua, FL, USA).

2.3 Single unit recordings with silicon multichannel electrodes

Silicon multichannel electrode probes (a4×4-3mm100-177, NeuroNexus Technologies, Ann Arbor, MI, USA) were inserted into the brainstem (see Figs. 1A, 1B). Signals were digitized (25 kHz) using up to four preamplifiers (RA16PA, Tucker-Davis Technologies, Alachua, FL, USA), and then synchronized and band-pass filtered (300–7,500 Hz) using a digital signal processor (RX5BA-5, Tucker-Davis Technologies, Alachua, FL, USA). Both the XII nerve and multichannel recording signals were acquired and analyzed using a custom in-house program written in MATLAB® (MathWorks, Inc., Natick, MA, USA).

2.4 Chemicals and drugs

All drugs and chemicals were obtained from Sigma/RBI Aldrich (St Louis, MO, USA) except for bicuculline, which was obtained from R&D Systems (Minneapolis, MN, USA). The synaptic transmission blockade solution consisted of aCSF solution with 50 μM CNQX (AMPA/kainate receptor antagonist; 6-cyano-7-nitroquinoxaline-2,3-dione), 50 μM APV (NMDA receptor antagonist; (2*R*)-amino-5-phosphonovaleric acid), 25 μM strychnine (glycine receptor antagonist), and 25 μM bicuculline ($GABA_A$ channel antagonist). This combination of receptor antagonist drugs is commonly used to test for intrinsically bursting neurons (e.g., Peña et al., 2004). The synaptic inhibition blockade solution consisted of aCSF solution with 25 μM strychnine and either 25 μM bicuculline or 20 μM picrotoxin ($GABA_A$ channel blocker). This solution was previously used to bathe isolated turtle brainstems and transform the rhythmic motor output (Johnson et al., 2007).

2.5 Experimental protocols

Brainstem preparations were allowed to equilibrate for 2–4 h before initiating a protocol. The pia mater was dissected away and silicon multichannel electrode probes were inserted into the brainstem. Once respiratory neurons (neurons firing in phase with XII motor bursts) were observed and a stable XII nerve signal achieved, baseline data were recorded for at least 2 h. The bath aCSF solution was switched to synaptic transmission blockade solution and data were recorded. At 2–6 h after the switch, when all spontaneous depolarizations on XII were abolished, any neuron firing bursts of action potentials was considered to have intrinsic bursting properties. After recording for 45–60 min with bath [KCl] = 3.0 mM, the bath [KCl] was sequentially increased to 6.0 and 9.0 mM and recordings obtained for 45–60 min at each concentration. In separate experiments, respiratory neurons were recorded before switching to synaptic inhibition blockade solution for 60 min.

2.6 Data analysis

Action potentials were obtained from band-pass filtered traces by clipping points for a 3 ms window prior to and following where the trace crossed a given voltage threshold. These tentative action potentials were compared and categorized according to their shapes defined by time and voltage. Action potentials with similar shapes were sorted into a group (Adamos et al., 2008). This technique allowed noise to be removed and multiple units to be separated

which were recorded on a single site. Auto- and cross-correlation histograms were examined to rule out waveforms as noise or one neuron being captured on two different recording sites. After sorting and identifying action potentials, each action potential was considered simply as a timestamp without any further reference to the voltage trace.

To determine the temporal firing pattern of respiratory neurons relative to the XII motor burst, cycle-triggered histograms were generated by averaging action potential times within 0.5 s bins for 10–25 breathing cycles (Fig. 2). Where possible, the XII motor bursts selected for cycle-triggered histograms were mostly singlet bursts with a stereotypical pattern for that particular brainstem (e.g., bursts with large rare large amplitude deflections during the burst were excluded from analysis). If the brainstem expressed all doublet XII motor bursts, the first burst was used to calculate the cycle-triggered histogram. These histograms were used to classify respiratory neurons based on the timing of the average peak firing rate and time when most action potentials fired. The classification scheme proposed by Takeda et al. (1986) was used to guide neuron classification (see first column of Table 1). The first two-thirds of the respiratory XII motor burst was considered the expiratory phase, while the last third of the XII burst was considered the inspiratory phase, based on the activity pattern for turtle brainstems under *in vitro* conditions (Johnson and Mitchell, 1998). Action potential firing prior to or at the onset of the XII motor burst was considered pre-expiratory (Pre-E), while action potential firing at the end or immediately after the XII motor burst was considered post-inspiratory (Post-I). For intrinsically bursting neurons, the number of spikes/burst, burst duration, and interval between bursts was quantified for 10 representative bursts. Data are reported as mean ± standard deviation.

3. Results

3.1 Respiratory neuron classification and location

While recording respiratory motor output on XII nerves in isolated adult turtle brainstems (n=15), silicon multichannel recording electrodes were placed in the brainstem lateral to the midline on either side. Respiratory (n=219) and non-respiratory neurons (n=6) were recorded in the brainstem in an area extending from caudal to the XII nerve root to caudal to the vestibulocochlear (VIII) and abducens (VI) nerve roots (Table 1; Fig. 3). Expiratory “E-cells” fired action potentials almost exclusively during the expiratory phase (Fig. 2A), while EI-cells had action potentials that fired substantially throughout the expiratory and inspiratory phases (Fig. 2B). These expiratory cells (n=183) were the most commonly found respiratory neurons and represented 84% of the total population (Table 1). Inspiratory “I-cells” (n=6) had peak firing rates during the last one-third of the XII motor discharge with low firing rates during all other phases (Fig. 2C; Table 1).

Post-inspiratory neurons (Post-I-cells; n=3) had a distinctive peak firing rate at the end of the XII motor burst (Fig. 2D). Other Post-I-cells had additional discharge during the expiratory phase and were classified as E-cell/Post-I-cells (n=11; Fig. 2E). Finally, respiratory neurons with peak discharge prior to onset of the XII motor burst were classified as Pre-E-cells (n=9; Fig. 2F). Post-I-cells and Pre-E-cells represented only 11% of the total population (Table 1). Other neurons (n=7) clearly fired action potentials in phase with the XII motor burst or were inhibited during the XII motor phase, but their average firing rate

was too low to allow them to be classified (referred to as respiratory-related units). The average peak firing rates for all respiratory neuron classes ranged between 2.5 and 17.9 Hz with the highest firing rates at 53 Hz (EI-cells in Table 1).

This study was not intended to generate a highly accurate three-dimensional, respiratory neuron density map of the turtle respiratory control network. Instead, the rostrocaudal location of electrode placement was marked on representative diagrams of turtle brainstems, but electrode angle and depth were not measured. Accordingly, the maps show that E-cells were primarily between the XII and X nerve roots, while EI-cells were also abundant in this area and extended rostral to the X nerve root at the level of the glossopharyngeal (IX) nerve root (Figs. 3A, 3B). I-cells were distributed in the area rostral to the XII nerve root up to the level of the IX root (Fig. 3C). Post-I-cells, E-cell/Post-I-cells, and Pre-E-cells were found mainly at the level of the X nerve root (Figs. 3D, 3E, 3F).

3.2 Characterization of respiratory neurons with intrinsic bursting properties

In eleven brainstems, the bath solution was switched to synaptic blockade solution (containing CNQX, APV, strychnine, bicuculline) to block fast excitatory glutamatergic and inhibitory GABA/glycine synaptic transmission. Synaptic blockade solution application disrupted respiratory motor output from the XII nerve within minutes. However, synchronized bursts of action potentials coinciding with small XII motor bursts were occasionally observed to persist for up to several hours following the switch to synaptic blockade solution. These small XII motor bursts would occur every 15–30 min and decrease in amplitude until they were abolished. When the XII motor bursts were completely abolished, any previously recorded neuron that exhibited bursts of action potentials was considered to have intrinsic bursting properties. Thus, a total of 19/182 (~10%) of respiratory and 3/6 non-respiratory neurons (data not shown) exhibited intrinsic bursting properties (Figs. 4A–4D).

At $[K^+]$ = 3 mM, only one I-cell had intrinsic bursting properties (43.9 spikes/burst, 3.4 s burst duration, 31.5 s between bursts). At $[K^+]$ = 6 mM, three respiratory neurons (EI-cell, I-cell, respiratory-related unit) had bursts of action potentials with an average of 31.1 ± 24.0 spikes/burst lasting 4.4 ± 3.9 s with 33.8 ± 5.9 s between bursts. At $[K^+]$ = 9 mM, eight expiratory cells (3 E-cells, 5 EI-cells), six post-inspiratory cells (2 Post-I-cells, 4 E-cell/Post-I-cells), one Pre-E-cell, and three respiratory-related units had bursts of action potentials with an average of 22.2 ± 28.1 spikes/burst lasting 2.3 ± 3.1 s with 16.3 ± 22.9 s between bursts. Post-inspiratory neurons had the highest percentage of neurons with intrinsic bursting properties (6/9, 67%). Intrinsically-bursting respiratory neurons were clustered in the region rostral to the XII nerve root and at the level of the X nerve root (Fig. 4E).

3.3 Synaptic inhibition blockade causes seizure-like activity

To test whether persistent rhythmic activity during synaptic inhibition blockade was due to seizure-like activity, simultaneous recordings from XII, IX, and V nerve roots were taken from turtle brainstems (n=2) prior to and during synaptic inhibition blockade. Within 20 min, bath-applied picrotoxin and strychnine produced large synchronized bursts of activity on all recorded nerve roots (Figs. 5A). Similar large bursts of activity that were

synchronized with XII bursts were recorded on VI, VII, VIII, and X nerve roots (data not shown). To examine neuronal firing patterns under similar conditions, silicon multichannel electrodes were placed in turtle brainstems (n=4) and baseline recordings of respiratory neurons were performed prior to bath-application of picrotoxin and strychnine. Under these conditions, synchronized, high frequency bursts of activity were observed on all multichannel recordings, even when one electrode was placed in the pons (Figs. 5B). Thus, the rhythmic motor activity during synaptic blockade was not related to respiratory activity, but instead represented seizure-like activity.

4. Discussion

The main findings were that ~10% of respiratory neurons in isolated turtle brainstems have intrinsic bursting properties. These neurons were distributed within several different classes of respiratory neurons with post-inspiratory neurons having the highest percentage of neurons expressing these properties. Most of the intrinsically bursting respiratory neurons were clustered at the level of the X nerve root. This study also expanded the scope of previously recorded respiratory neurons in turtles and demonstrated a rich diversity of firing patterns in the brainstem. Finally, we showed that synaptic inhibition blockade produced seizure-like activity in turtle brainstems, thereby casting doubt as to whether this experimental approach can be used to argue for the existence of respiratory neurons with intrinsically bursting properties.

4.1 Activity patterns and location of respiratory neurons in turtle brainstems

The respiratory control network in the turtle brainstem is poorly understood. To our knowledge, only one other study recorded respiratory neurons in the brainstem of decerebrated turtles using sharp intracellular recording techniques (Takeda et al., 1986). In that study, forty-three neurons recorded at the level of cranial nerve X roots were classified as E neurons (expiratory, 27/43), I neurons (inspiratory, 9/43), and PI neurons (post-inspiratory, 7/43), with examples shown of a pi-E neuron (post-inspiratory-expiratory [analogous to E-cell/Post-I-cell in this study]) and an E-I neuron (expiratory-inspiratory [analogous to an EI-cell in this study]). There was no indication of cell numbers or localization for the pi-E or E-I cells. The authors correlated the firing patterns of these respiratory neuron classes with specific muscle firing patterns (Gans and Hughes, 1967), such as E neurons (pectoralis muscle, expiratory), pi-E neurons (transverse abdominal muscle), E-I neurons (glottal abductor muscle), PI neurons (glottal adductor activity), and I neurons (serratus muscle, inspiratory) (Takeda et al., 1986). Another key finding in their study was that E neurons undergo gradual depolarization prior to the onset of the expiratory phase, but the existence of Pre-E neurons was not confirmed. Our results are similar in that E-cells were the most commonly found respiratory neurons, and representative neurons from all of the previously described classes were found. This study extends these results by demonstrating that respiratory neurons are found more rostral in the medulla and revealed Pre-E-cells, which were proposed to exist by Takeda et al. (1986). In addition, the peak firing rates for the different classes of respiratory neurons were quantified in this study, thereby giving some indication as the relative activity of the respiratory neurons in isolated turtle brainstems.

There are several caveats to our experimental results. First, we recognize that classifying respiratory neurons is fraught with difficulty because respiratory neuron firing is variable from cycle to cycle, and there is a continuum between classes of respiratory neurons (Carroll and Ramirez, 2013; Carroll et al., 2013). Although classification schemes do not predict neuronal function within the respiratory network, they do provide a working framework and descriptive vocabulary for developing future hypotheses. A second caveat is the variability in the XII motor output, which made classification difficult if not impossible in some cases (these data were not included in this study). Also, the number of XII motor bursts for analysis was relatively low compared to studies using anesthetized mammals. To circumvent both of these problems, $5HT_3$ or α1-adrenergic receptor agonist drugs could be used in future studies to produce highly regular robust singlet XII motor bursts (Bartman et al., 2010). Finally, the synaptic blockade solution used in this study was not designed to block electrical synapses between neurons. It is possible that some neurons were still electrically-coupled during synaptic blockade conditions. The slow, infrequent depolarizations that we observed during the first few hours of synaptic blockade may have been due spontaneous depolarizations among electrically-coupled neurons. Although we cannot rule out definitively whether neurons were still electrically-coupled, there was no evidence of coincident neuronal firing while recording from 32 channels when intrinsic bursting properties were revealed.

Given the dynamic and stochastic nature of respiratory rhythm generation (Carroll and Ramirez, 2013), the function of different respiratory neurons is speculative. In addition to the neuronal functions proposed by Takeda et al. (1986), we agree with Takeda et al. (1986) that the initiation of expiration is an important feature of turtle (reptilian) respiratory rhythm generation since red-eared slider turtles have a typically prolonged post-inspiratory phase following several cycles of expiration and inspiration (Gans and Hughes, 1967; Milsom and Jones, 1980). Thus, the Pre-E-cells identified in this study are candidate neurons for initiating expiration because they fire prior to the onset of a respiratory burst. We hypothesize that these different Pre-E-cells are connected to other Pre-E-cells and E-cells via excitatory glutamatergic synapses to increase excitation within the turtle respiratory rhythm generator to begin the expiratory phase. Post-I-cells may be important for terminating inspiration and allowing expiration to occur within a breathing episode, as well as terminating an episode of several consecutive cycles of expiratory and inspiratory activity. Excitation of Post-I-cells may enhance episode termination and transform episodic breathing into singlet breathing. In isolated turtle brainstems, bath-applied $5HT_3$ receptor agonist drugs increase singlet breathing while $5HT_3$ receptor antagonist drugs increase episodic breathing (Bartman et al., 2010). Similarly, hypoxia-induced singlet breathing in intact turtles is abolished by pretreatment with $5HT_3$ receptor antagonist drugs (S.M. Johnson, A.R. Krisp, M.E. Bartman, unpublished observations). Thus, we hypothesize that a subpopulation of Post-I-cells are depolarized by activation of postsynaptic $5HT_3$ receptors to terminate inspiration and reduce episodic breathing.

4.2 Intrinsic bursting properties of neurons in respiratory motor control

The question as to whether intrinsically bursting respiratory neurons properties play a role in vertebrate respiratory rhythm generation was controversial for many years (Del Negro et al.,

2008; Ramirez et al., 2011; Carroll and Ramirez, 2013). Respiratory neurons with intrinsic bursting properties were identified and incorporated into mechanistic computational models for respiratory rhythm generation in neonatal rodents. Experimental evidence suggested that intrinsically bursting respiratory neurons were not necessary for rhythm generation (Del Negro et al., 2005). Since experimental methods do not currently exist for specifically inactivating the specific ionic currents underlying intrinsic bursting properties in respiratory neurons, attention was redirected towards alternative mechanisms underlying rhythmogenesis. A recent compelling hypothesis is that excitatory glutamatergic synaptic transmission in the dendrites of preBötC neurons triggers postsynaptic calcium-activated calcium currents that initiate a powerful wave of excitation towards the cell soma, resulting in the distinctive respiratory depolarization and burst of action potentials (Rekling and Feldman, 1998; Del Negro et al., 2002; Feldman et al., 2003; Mironov, 2008; Del Negro et al., 2010).

Are there other roles that intrinsically bursting respiratory neurons play in respiratory motor control? One hypothesis is that during severe hypoxia, a specific subclass of intrinsically bursting respiratory neurons (with persistent sodium currents) is critical for generating gasping motor behavior (Peña et al., 2004; Paton et al., 2006; Peña and Aguileta, 2007; Smith et al., 2007, 2013), suggesting that the importance of intrinsically bursting neurons is state-dependent. A second hypothesis is that intrinsically bursting neurons increase the robustness of the respiratory network (Purvis et al., 2006, 2007) by providing stability and non-linear amplification (Carroll and Ramirez, 2013). In a computational model of the neonatal rat preBötC, the largest increase in dynamic range occurs when the number of intrinsically bursting neurons is greater than 20% of the population (Purvis et al., 2007). Finally, a third perspective hypothesizes that respiratory rhythm generation is the product of complex and highly modulated interactions between synaptic transmission and neuronal membrane properties. Intrinsic bursting properties in respiratory neurons may represent one of several rhythmogenic mechanisms that work together to produce breathing (Ramirez et al., 2011, 2012; Lindsey et al., 2012).

Despite the intensive effort to characterize underlying mechanisms and construct computational models (reviewed in Lindsey et al., 2012), there is little experimental evidence to support or refute the question as to whether intrinsically bursting neurons are found in adult vertebrates, and whether these neurons play a key role in respiratory rhythm generation. This is primarily due to the daunting technical challenges associated with studying neuronal properties in adult mammals. To our knowledge, this type of experiment was performed once in young P14-P21 rodents using the versatile working-heart brainstem preparation (St John et al., 2009). In their study, respiratory neurons were identified in the preBötC and the rostral ventral respiratory group, ~21% (14/66) of respiratory neurons expressed intrinsic bursting properties. The authors hypothesized that these neurons are “released” during severe hypoxia to generate gasping motor behavior (St John et al., 2009). Finding intrinsically bursting respiratory neurons in juvenile rats is an important advance because it demonstrates that these neurons exist in animals older than neonates. However, juvenile P14-P21 rats are near the age of weaning, have not gone through puberty, and are not fully mature adults capable of reproduction.

Accordingly, testing for intrinsically bursting respiratory neurons in adult turtles allows the question to be addressed in a fully mature ectothermic vertebrate at physiological temperatures and conditions. In the current study, ~10% of identified respiratory neurons with intrinsic bursting properties were found throughout an extended region of the turtle medulla. The fact that most of the intrinsically bursting neurons were revealed when bath [K^+] was increased to 6–9 mM may mean that intrinsically bursting neurons are silent during normal bath potassium levels ([K^+] = 3–5 mM). On the other hand, it may be necessary to increase bath [K^+] to replace the lost excitatory synaptic inputs due to the presence of APV and CNQX during synaptic transmission blockade. Intrinsic bursting properties were especially abundant in post-inspiratory neurons (Post-I-cells, E-cell/Post-I-cells), but the significance of this finding is not clear. It's possible that post-inspiratory neurons are inhibited during inspiration and have intrinsic membrane conductances that produce a strong rebound depolarization following inspiration to close the glottis prior to breathholding. Under conditions of synaptic transmission blockade, these conductances may be responsible for generating bursts of action potentials. Accordingly, the next logical step would be to characterize the ionic mechanisms underlying intrinsic bursting in turtle respiratory neurons.

In the preBötC of neonatal rodents, persistent sodium (riluzole-sensitive) or calcium-activated cation currents (flufenamic acid-sensitive) are responsible for the intrinsic bursting properties (Thoby-Brisson and Ramirez, 2001). In isolated brainstems from red-eared slider turtles, respiratory motor output is relatively unaltered by riluzole and abolished with increasing concentrations of bath-applied flufenamic acid (Johnson et al., 2007). We hypothesized that there are no riluzole-sensitive intrinsically bursting respiratory neurons since this turtle species does not appear to express gasping during severe hypoxia (Johnson et al., 2007). The lack of gasping is confirmed when turtles are allowed to breathe 100% nitrogen gas for 4 h (S.M. Johnson, A.R. Krisp, M.E. Bartman, unpublished observations). Thus, we hypothesize that intrinsically bursting respiratory neurons in red-eared slider turtles are sensitive only to flufenamic acid. In other species, however, this may not be the case because lung burst frequency is decreased by both riluzole and flufenamic acid in isolated brainstems from post-metamorphic frogs (M.S. Hedrick, unpublished observations).

4.3 Advantages and caveats with multichannel recording in isolated turtle brainstems

Multichannel recordings of respiratory neurons in the brainstem are used extensively in anesthetized cats (Lindsey et al., 2000; Morris et al., 2003) and more recently in rhythmically active murine medullary slices (Carroll and Ramirez, 2013; Carroll et al., 2013). This is the first study to use silicon multichannel recording electrodes to identify respiratory neurons in isolated adult vertebrate brainstems under *in vitro* conditions. Multichannel recording techniques allow many single unit recordings of respiratory neurons to be isolated at one time at different tissue depths. Intracellular recording provides detailed information on current-voltage relationships within a single neuron, but is very laborious and requires considerable amounts of time to record from large numbers of neurons. Alternative methods of recording respiratory neuron populations, such as the use of voltage-sensitive (Onimaru and Homma, 2003) or calcium-sensitive dyes (Koshiya and Smith, 1999) are limited because only neurons close to the tissue surface can be visualized. In addition, it

is difficult to resolve individual neurons using optical methods and the dyes used for imaging active neurons may profoundly alter respiratory network activity.

The limitations of the multichannel recording techniques used in this study are that only a limited number of electrodes could be placed in the tissue without disrupting network activity due to mechanical perturbations of the tissue. This limited the area and number of respiratory neurons that could be identified and tested for intrinsic bursting properties. Also, the exact position of recording sites on silicon multichannel electrodes was not easy to quantify given the complex geometry of the electrode. In contrast, it is much easier to determine the position and depth of a single electrode tip using a stereotaxic apparatus, or the location of a glass electrode tip can be localized if the electrode is filled with a dye that can be ejected from the tip. Another caveat is that the recording sites on the silicon multichannel electrodes cannot be moved individually to optimize neuronal recordings. In contrast, multichannel recordings in anesthetized cats can be performed with multiple, separately controlled recording electrodes that can be moved to increase signal strength (e.g., Segers et al., 2008).

4.4 Respiratory motor control in reptiles and other vertebrates

Among ectothermic vertebrates, it is challenging to identify evolutionarily conserved neuronal phenotypes and network properties, such as rhythm generating sites, neurotransmitter receptor phenotypes (e.g., neurokinin and mu-opioid receptors), and mechanistic features (e.g., role of synaptic inhibition or intrinsically bursting neurons, specific rhythm generation mechanisms) (Hedrick, 2005; Wilson et al., 2006; Kinkead, 2009; Milsom, 2010). Recent reviews reveal that most work has been performed on lamprey (e.g., Bongianni et al., 2014) and frogs (e.g., Gargaglioni and Milsom, 2007). With respect to site of rhythm generation, there is wide variation in ectothermic vertebrates. In lamprey brainstems, a site rostral to the trigeminal nucleus (pTRG, paratrigeminal respiratory group) appears to contain the respiratory central pattern generator for gill ventilatory movements (Mutolo et al., 2007). In contrast, the site of rhythm generation in frogs is complex because of the existence of two distinct oscillators controlling buccal and lung ventilation (Vasilakos et al., 2006; Wilson et al., 2002, 2006; Duchcherer et al., 2013). In reptiles, the site of respiratory rhythm generation is completely unknown. The present study and Takeda et al. (1986) reveal a large distribution of respiratory neurons in the turtle medulla, but no one has targeted a specific region with lesions or chemical injections to test whether that site was necessary for rhythm generation, expiratory activity, or inspiratory activity.

With respect to specific neurotransmitter responses and phenotypes, respiratory motor output produced by lamprey and frog brainstems is inhibited by mu-opioid receptor activation (Mutolo et al., 2007; Davies et al., 2009) and excited by neurokinin receptor activation (Chen and Hedrick, 2008; Mutolo et al., 2010). In contrast, respiratory motor output from isolated turtle brainstems is inhibited by mu-opioid receptor activation (Johnson et al., 2010), but oddly insensitive to bath-applied substance P (S.M. Johnson, unpublished observations). Thus, there is significant variability in turtle responses compared to lamprey and frogs. The role of synaptic inhibition in lamprey and frog respiratory rhythm generation appears to be similar to turtles (Johnson et al., 2002) in that rhythmic activity persists during

synaptic inhibition blockade (Rovainen, 1983; Galante et al., 1996; Broch et al., 2002). However, potentially important differences exist that may be due to species differences and combinations/concentrations of bath-applied drugs. For example, synaptic inhibition blockade with bicuculline and strychnine (or picrotoxin) at 20–25 μM induced widespread seizure-like activity in turtle brainstems in this study. In contrast, seizure-like activity is induced only sporadically in isolated lamprey brainstems with bicuculline and strychnine (10 μM each) (Fig. 2 in Bongianni et al., 2006). Also, these irregular seizure-like bursts are abolished when glutamatergic receptor antagonist drugs are also bath-applied (Fig. 4 in Mutolo et al., 2011), suggesting that the respiratory rhythm is transformed under these conditions and not overwhelmed by widespread rhythmic bursts of neuronal activity. Thus, different responses to neurotransmitter receptor antagonist drugs may reflect differences in underlying rhythm generating mechanisms and thresholds for inducing seizure-like bursts of neuronal activity within isolated brainstems. The previously described “group pacemaker” model is hypothesized to explain rhythm generation in lamprey (Mutolo et al., 2010) and turtle (Johnson et al., 2007) based on results from bath-application of riluzole and flufenamic acid to isolated brainstems. However, these drugs are not highly specific for the ionic currents proposed to underlie rhythm generation, suggesting that these data need to be interpreted cautiously.

In summary, reptiles are unique among vertebrates in that they aspirate air into their lungs by activating spinal motoneurons, similar to mammals. Unlike mammals, however, many reptiles have breathing episodes initiated by expiratory activity with long post-inspiratory apneas in between breathing episodes. Likewise, frogs pump air into their lungs using buccal musculature while lamprey use brachial muscles to force water out of gill openings. Thus, there may be some similarities in anatomical and physiological function of respiratory control networks in these vertebrate classes, but divergence in neuronal mechanisms and neurotransmitter responses may be more prevalent due to their widely variant habitats and ventilatory strategies.

Compared to lamprey and amphibians, our understanding of reptilian respiratory rhythm generation and control lags far behind, making it difficult to compare and contrast studies. In reptiles, there is a need to further map the respiratory control network, and test network responses to localized neurotransmitter application to identify rhythmogenic sites. The isolated turtle brainstem is an ideal model for such studies in reptiles because the tissue is hypoxia-resistant and capable of producing respiratory motor output (similar to intact turtles) under *in vitro* conditions for days (Wilkerson et al., 2003).

Acknowledgments

This work was supported by the National Science Foundation (IOB 0517302 to SMJ), American Physiological Society (Research Career Enhancement Award to MSH), and National Institutes of Health (NIH T32 GM007507 to BMK).

References

Adamos DA, Kosmidis EK, Theophilidis G. Performance evaluation of PCA-based spike sorting algorithms. Comput Methods Programs Biomed. 2008; 91:232–244. [PubMed: 18565614]

Bartman ME, Wilkerson JE, Johnson SM. 5-HT_3 receptor-dependent modulation of respiratory burst frequency, regularity, and episodicity in isolated adult turtle brainstems. Respir Physiol Neurobiol. 2010; 172:42–52. [PubMed: 20399913]

Bongianni F, Mutolo D, Cinelli E, Pantaleo T. Neural mechanisms underlying respiratory rhythm generation in the lamprey. Respir Physiol Neurobiol. 2014 Epub ahead of print.

Bongianni F, Mutolo D, Nardone F, Pantaleo T. GABAergic and glycinergic inhibitory mechanisms in the lamprey respiratory control. Brain Res. 2006; 1090:134–145. [PubMed: 16630584]

Broch L, Morales RD, Sandoval AV, Hedrick MS. Regulation of the respiratory central pattern generator by chloride-dependent inhibition during development in the bullfrog (*Rana catesbeiana*). J Exp Biol. 2002; 205:1161–1169. [PubMed: 11919275]

Butera RJ, Rinzel J, Smith JC. Models of respiratory rhythm generation in the pre-Bötzinger complex. I Bursting pacemaker neurons. J Neurophysiol. 1999a; 81:382–397. [PubMed: 10400966]

Butera RJ, Rinzel J, Smith JC. Models of respiratory rhythm generation in the pre-Bötzinger complex. II Populations of coupled pacemaker neurons. J Neurophysiol. 1999b; 81:398–415. [PubMed: 10400967]

Carroll MS, Ramirez JM. Cycle-by-cycle assembly of respiratory network activity is dynamic and stochastic. J Neurophysiol. 2013; 109:296–305. [PubMed: 22993257]

Carroll MS, Viemari JC, Ramirez JM. Patterns of inspiratory phase-dependent activity in the in vitro respiratory network. J Neurophysiol. 2013; 109:285–295. [PubMed: 23076109]

Chapman MA, Johnson SM. Respiratory-related pacemaker neurons in isolated turtle brainstems in vitro. The FASEB Journal. 2008:Abstract #1628.

Chen AK, Hedrick MS. Role of glutamate and substance P in the amphibian respiratory network during development. Respir Physiol Neurobiol. 2008; 162:24–31. [PubMed: 18450524]

Cruce WL, Nieuwenhuys R. The cell masses in the brain stem of the turtle Testudo hermanni; a topographical and topological analysis. J Comp Neurol. 1974; 156:277–306. [PubMed: 4418301]

Davies BL, Brundage CM, Harris MB, Taylor BE. Lung respiratory rhythm and pattern generation in the bullfrog: role of neurokinin-1 and mu-opioid receptors. J Comp Physiol B. 2009; 179:579–592. [PubMed: 19184042]

Del Negro CA, Hayes JA, Pace RW, Brush BR, Teruyama R, Feldman JL. Synaptically activated burst-generating conductances may underlie a group-pacemaker mechanism for respiratory rhythm generation in mammals. Prog Brain Res. 2010; 187:111–136. [PubMed: 21111204]

Del Negro CA, Morgado-Valle C, Feldman JL. Respiratory rhythm: an emergent network property? Neuron. 2002; 34:821–830. [PubMed: 12062027]

Del Negro CA, Morgado-Valle C, Hayes JA, Mackay DD, Pace RW, Crowder EA, Feldman JL. Sodium and calcium current-mediated pacemaker neurons and respiratory rhythm generation. J Neurosci. 2005; 25:446–453. [PubMed: 15647488]

Del Negro CA, Pace RW, Hayes JA. What role do pacemakers play in the generation of respiratory rhythm? Adv Exp Med Biol. 2008; 605:88–93. [PubMed: 18085252]

Duchcherer M, Baghdadwala MI, Paramonov J, Wilson RJ. Localization of essential rhombomeres for respiratory rhythm generation in bullfrog tadpoles using a binary search algorithm: Rhombomere 7 is essential for the gill rhythm and suppresses lung bursts before metamorphosis. Dev Neurobiol. 2013; 73:888–898. [PubMed: 23843256]

Feldman, JL.; Cleland, CL. Possible roles of pacemaker neurons in mammalian respiratory rhythmogenesis. In: Carpenter, DO., editor. Cellular pacemakers. New York: 1982. p. 101-119.

Feldman JL, Del Negro CA. Looking for inspiration: new perspectives on respiratory rhythm. Nat Rev Neurosci. 2006; 26:232–242. [PubMed: 16495944]

Feldman JL, Del Negro CA, Gray PA. Understanding the rhythm of breathing: so near, yet so far. Annu Rev Physiol. 2013; 75:423–452. [PubMed: 23121137]

Feldman JL, Mitchell GS, Nattie EE. Breathing: rhythmicity, plasticity, chemosensitivity. Annu Rev Neurosci. 2003; 26:239–266. [PubMed: 12598679]

Funk GD, Feldman JL. Generation of respiratory rhythm and pattern in mammals: insights from developmental studies. Curr Opin Neurobiol. 1995; 5:778–785. [PubMed: 8805408]

Galante RJ, Kubin L, Fishman AP, Pack AI. Role of chloride-mediated inhibition in respiratory rhythmogenesis in an in vitro brainstem of tadpole, *Rana catesbeiana*. J Physiol. 1996; 492:545–558. [PubMed: 9019549]

Gans C, Hughes GM. The mechanism of lung ventilation in the tortoise Testudo graeca linne. J Exp Biol. 1967; 47:1–20. [PubMed: 6058978]

Gargaglioni LH, Milsom WK. Control of breathing in anuran amphibians. Comp Biochem Physiol A Mol Integr Physiol. 2007; 147:665–684. [PubMed: 16949847]

Getting, PA. Comparative analysis of invertebrate central pattern generators. In: Cohen, AH.; Rossignol, S.; Grillner, S., editors. Neural control of rhythmic movements in vertebrates. New York: 1988. p. 101-127.

Hedrick MS. Development of respiratory rhythm generation in ectothermic vertebrates. Respir Physiol Neurobiol. 2005; 149:29–41. [PubMed: 15914099]

Jackson DC. Living without oxygen: lessons from the freshwater turtle. Comp Biochem Physiol A Mol Integr Physiol. 2000; 125:299–315. [PubMed: 10794959]

Johnson SM, Johnson RA, Mitchell GS. Hypoxia, temperature, and pH/CO_2 effects on respiratory discharge from a turtle brain stem preparation. J Appl Physiol. 1998; 84:649–660. [PubMed: 9475877]

Johnson SM, Mitchell GS. N-methyl-D-aspartate-mediated bulbospinal respiratory drive is pH/P(CO2)-insensitive in turtle brainstem-spinal cord. Respir Physiol. 1998; 113:201–212. [PubMed: 9840329]

Johnson SM, Moris CM, Bartman ME, Wiegel LM. Excitatory and inhibitory effects of opioid agonists on respiratory motor output produced by isolated brainstems from adult turtles (*Trachemys*). Respir Physiol Neurobiol. 2010; 170:5–15. [PubMed: 19833235]

Johnson SM, Smith JC, Funk GD, Feldman JL. Pacemaker behavior of respiratory neurons in medullary slices from neonatal rat. J Neurophysiol. 1994; 72:2598–2608. [PubMed: 7897477]

Johnson SM, Wiegel LM, Majewski DJ. Are pacemaker properties required for respiratory rhythm generation in adult turtle brain stems in vitro? Am J Physiol Regul Integr Comp Physiol. 2007; 293:R901–R910. [PubMed: 17522127]

Johnson SM, Wilkerson JE, Wenninger MR, Henderson DR, Mitchell GS. Role of synaptic inhibition in turtle respiratory rhythm generation. J Physiol. 2002; 544:253–265. [PubMed: 12356896]

Kinkead R. Phylogenetic trends in respiratory rhythmogenesis: insights from ectothermic vertebrates. Respir Physiol Neurobiol. 2009; 168:39–48. [PubMed: 19505591]

Koshiya N, Smith JC. Neuronal pacemaker for breathing visualized in vitro. Nature. 1999; 400:360–363. [PubMed: 10432113]

Lindsey BG, Morris KF, Segers LS, Shannon R. Respiratory neuronal assemblies. Respir Physiol. 2000; 122:183–196. [PubMed: 10967343]

Lindsey BG, Rybak IA, Smith JC. Computational models and emergent properties of respiratory neural networks. Compr Physiol. 2012; 2:1619–1670. [PubMed: 23687564]

Milsom WK. Adaptive trends in respiratory control: a comparative perspective. Am J Physiol Regul Integr Comp Physiol. 2010; 299:R1–R10. [PubMed: 20357023]

Milsom WK, Jones DR. The role of vagal afferent information and hypercapnia in control of the breathing pattern in chelonia. J Exp Biol. 1980; 87:53–63. [PubMed: 7420020]

Mironov SL. Metabotropic glutamate receptors activate dendritic calcium waves and TRPM channels which drive rhythmic respiratory patterns in mice. J Physiol. 2008; 586:2277–2291. [PubMed: 18308826]

Morris KF, Baekey DM, Nuding SC, Dick TE, Shannon R, Lindsey BG. Invited review: Neural network plasticity in respiratory control. J Appl Physiol. 2003; 94:1242–1252. [PubMed: 12571145]

Mutolo D, Bongianni F, Cinelli E, Pantaleo T. Role of neurokinin receptors and ionic mechanisms within the respiratory network of the lamprey. Neuroscience. 2010; 169:1136–1149. [PubMed: 20540991]

Mutolo D, Bongianni F, Einum J, Dubuc R, Pantaleo T. Opioid-induced depression in the lamprey respiratory network. Neuroscience. 2007; 150:720–729. [PubMed: 17949922]

Mutolo D, Cinelli E, Bongianni F, Pantaleo T. Identification of a cholinergic modulatory and rhythmogenic mechanism within the lamprey respiratory network. J Neurosci. 2011; 31:13323–13332. [PubMed: 21917815]

Onimaru H, Arata A, Homma I. Firing properties of respiratory rhythm generating neurons in the absence of synaptic transmission in rat medulla in vitro. Exp Brain Res. 1989; 76:530–536. [PubMed: 2551710]

Onimaru H, Arata A, Homma I. Intrinsic burst generation of preinspiratory neurons in the medulla of brainstem-spinal cord preparations isolated from newborn rats. Exp Brain Res. 1995; 106:57–68. [PubMed: 8542977]

Onimaru H, Homma I. A novel functional neuron group for respiratory rhythm generation in the ventral medulla. J Neurosci. 2003; 23:1478–1486. [PubMed: 12598636]

Paton JF. Rhythmic bursting of pre- and post-inspiratory neurones during central apnoea in mature mice. J Physiol. 1997; 502:623–639. [PubMed: 9279813]

Paton JF, Abdala APL, Koizumi H, Smith JC, St-John W. Respiratory rhythm generation during gasping depends on persistent sodium current. Nat Neurosci. 2006; 9:311–313. [PubMed: 16474390]

Peña F, Aguileta MA. Effects of riluzole and flufenamic acid on eupnea and gasping of neonatal mice in vivo. Neurosci Lett. 2007; 415:288–293. [PubMed: 17276002]

Peña F, Parkis MA, Tryba AK, Ramirez JM. Differential contribution of pacemaker properties to the generation of respiratory rhythms during normoxia and hypoxia. Neuron. 2004; 43:105–117. [PubMed: 15233921]

Purvis LK, Smith JC, Koizumi H, Butera RJ. Intrinsic bursters increase the robustness of rhythm generation in an excitatory network. J Neurophysiol. 2007; 97:1515–1526. [PubMed: 17167061]

Purvis LK, Wright TM, Smith JC, Butera RJ. Significance of pacemaker vs. non-pacemaker neurons in an excitatory rhythmic network. Conf Proc IEEE Eng Med Biol Soc. 2006; 1:607–608. [PubMed: 17946408]

Ramirez JM, Doi A, Garcia AJ 3rd, Elsen FP, Koch H, Wei AD. The cellular building blocks of breathing. Compr Physiol. 2012; 2:2683–2731. [PubMed: 23720262]

Ramirez JM, Koch H, Garcia AJ, Doi A, Zanella S. The role of spiking and bursting pacemakers in the neuronal control of breathing. J Biol Phys. 2011; 37:241–261. [PubMed: 22654176]

Ramirez JM, Telgkakmp P, Elsen FP, Quellmalz UJA, Richter DW. Respiratory rhythm generation in mammals: synaptic and membrane properties. Resp Physiol. 1997; 110:71–85.

Rekling JC, Feldman JL. PreBötzinger complex and pacemaker neurons: hypothesized site and kernel for respiratory rhythm generation. Ann Rev Physiol. 1998; 60:385–405. [PubMed: 9558470]

Richter DW, Smith JC. Respiratory rhythm generation in vivo. Physiology. 2014; 29:58–71. [PubMed: 24382872]

Richter DW, Spyer KM. Studying rhythmogenesis of breathing: comparison of in vivo and in vitro models. Trends Neurosci. 2001; 24:464–472. [PubMed: 11476886]

Rovainen CM. Generation of respiratory activity by the lamprey brain exposed to picrotoxin and strychnine, and weak synaptic inhibition in motoneurons. Neurosci. 1983; 10:875–882.

Rubin JE, Hayes JA, Mendenhall JL, Del Negro CA. Calcium-activated nonspecific cation current and synaptic depression promote network-dependent burst oscillations. Proc Natl Acad Sci USA. 2009; 106:2939–2944. [PubMed: 19196976]

Segers LS, Nuding SC, Dick TE, Shannon R, Baekey DM, Solomon IC, Morris KF, Lindsey BG. Functional connectivity in the pontomedullary respiratory network. J Neurophysiol. 2008; 100:1749–1769. [PubMed: 18632881]

Smith JC, Abdala AP, Koizumi H, Rybak IA, Paton JF. Spatial and functional architecture of the mammalian brain stem respiratory network: a hierarchy of three oscillatory mechanisms. J Neurophysiol. 2007; 98:3370–3387. [PubMed: 17913982]

Smith JC, Abdala AP, Borgmann A, Rybak IA, Paton JF. Brainstem respiratory networks: building blocks and microcircuits. Trends Neurosci. 2013; 36:152–162. [PubMed: 23254296]

Smith JC, Butera RJ, Koshiya N, Del Negro C, Wilson CG, Johnson SM. Respiratory rhythm generation in neonatal and adult mammals: the hybrid pacemaker-network model. Resp Physiol. 2000; 122:131–147.

Smith JC, Ellenberger HH, Ballanyi K, Richter DW, Feldman JL. Pre-Bötzinger complex: a brainstem region that may generate respiratory rhythm in mammals. Science. 1991; 254:726–729. [PubMed: 1683005]

St-John WM, Stornetta RL, Guyenet PG, Paton JF. Location and properties of respiratory neurones with putative intrinsic bursting properties in the rat in situ. J Physiol. 2009; 587:3175–3188. [PubMed: 19417093]

Takeda R, Remmers JE, Baker JP, Madden KP, Farber JP. Postsynaptic potentials of bulbar respiratory neurons of the turtle. Resp Physiol. 1986; 64:149–160.

Thoby-Brisson M, Ramirez JM. Role of inspiratory pacemaker neurons in mediating the hypoxic response of the respiratory network in vitro. J Neurosci. 2000; 20:5858–5866. [PubMed: 10908629]

Thoby-Brisson M, Ramirez JM. Identification of two types of inspiratory pacemaker neurons in the isolated respiratory neural network of mice. J Neurophysiol. 2001; 86:104–112. [PubMed: 11431492]

Vasilakos K, Kimura N, Wilson RJ, Remmers JE. Lung and buccal ventilation in the frog: uncoupling coupled oscillators. Physiol Biochem Zool. 2006; 79:1010–1018. [PubMed: 17041867]

Wilkerson JE, Wenniger MR, Mitchell GS, Johnson SM. Time-dependent changes in spontaneous respiratory activity in turtle brainstems in vitro. Respir Physiol Neurobiol. 2003; 138:253–63. [PubMed: 14609514]

Wilson RJ, Vasilakos K, Harris MB, Straus C, Remmers JE. Evidence that ventilatory rhythmogenesis in the frog involves two distinct neuronal oscillators. J Physiol. 2002; 540:557–570. [PubMed: 11956343]

Wilson RJ, Vasilakos K, Remmers JE. Phylogeny of vertebrate respiratory rhythm generators: the Oscillator Homology Hypothesis. Respir Physiol Neurobiol. 2006; 154:47–60. [PubMed: 16750658]

Highlights

- Respiratory neurons were identified in adult turtle brainstems.
- Ten percent of respiratory neurons were intrinsically bursting neurons.
- Synaptic inhibition blockade resulted in seizure-like activity.
- Intrinsically bursting neurons may contribute to turtle breathing.

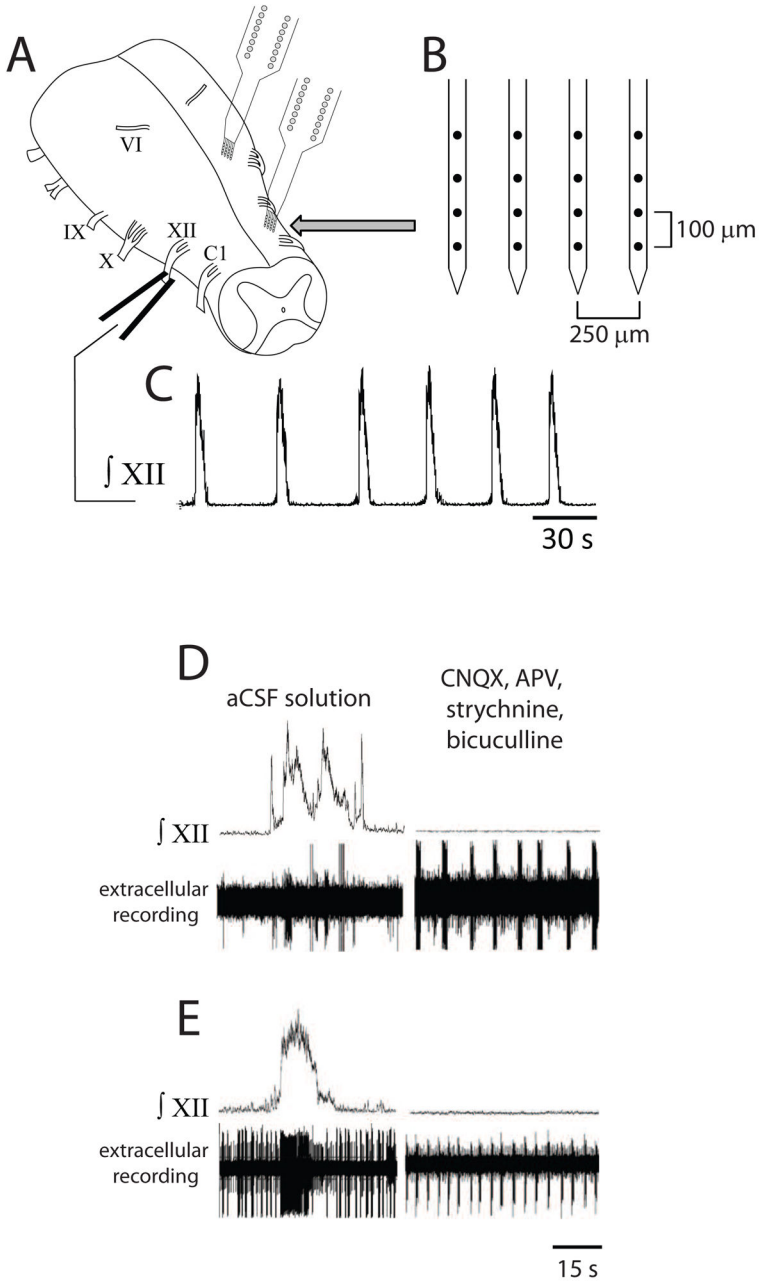

Fig. 1.

Multichannel recording in isolated turtle brainstem producing spontaneous respiratory motor output. (A) Drawing of turtle brainstem *in vitro* with suction electrode attached to XII nerve root and two silicon multichannel electrodes inserted into the brainstem. (B) Magnification of a single silicon multichannel electrode with four shanks (black circles on shanks represent recording sites). (C) Spontaneous respiratory motor output recorded on XII nerve root. (D, E) Integrated XII motor output and extracellular recordings from respiratory-related neurons under control conditions (aCSF solution; left panels) and during synaptic transmission blockade (right panels). Multiple neurons were recorded in aCSF solution and one neuron in

each case exhibited intrinsic bursting properties during synaptic transmission blockade (right panels).

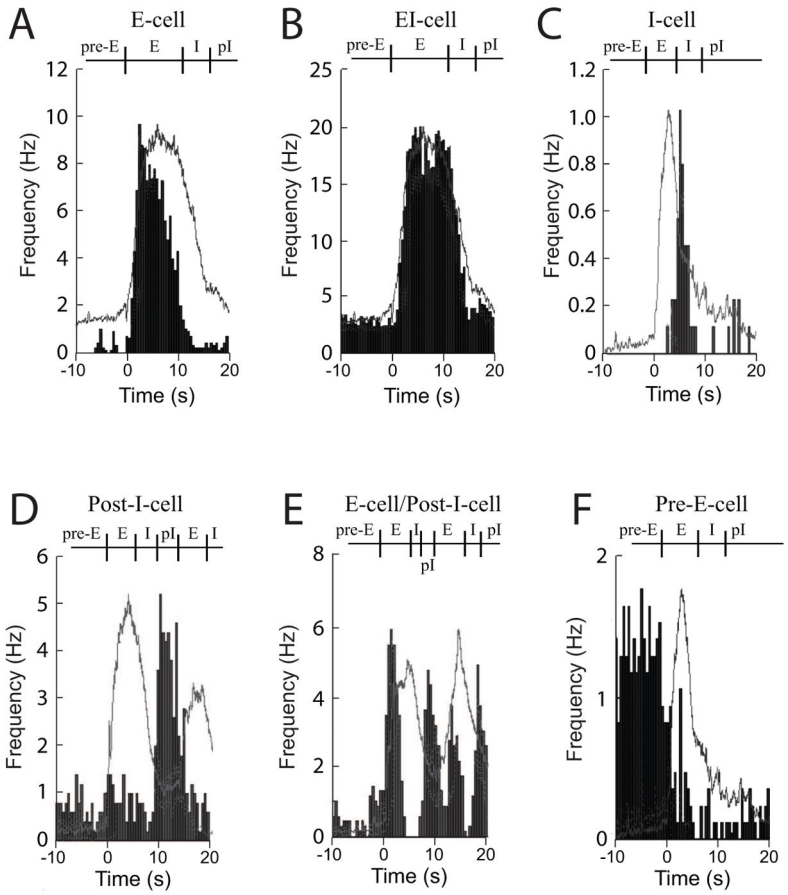

Fig. 2.

Cycle-triggered histograms are shown for two types of expiratory neurons, such as an E-cell (A) and EI-cell (B); an inspiratory neuron, such as an I-cell (C); two types of post-inspiratory cells, such as a Post-I-cell (D) and an E-cell/Post-I-cell; and a pre-expiratory cell, such as a Pre-E-cell (F). The light gray line represents the averaged XII respiratory motor burst with the average action potential frequency graphed in black histograms (0.5 s bins).

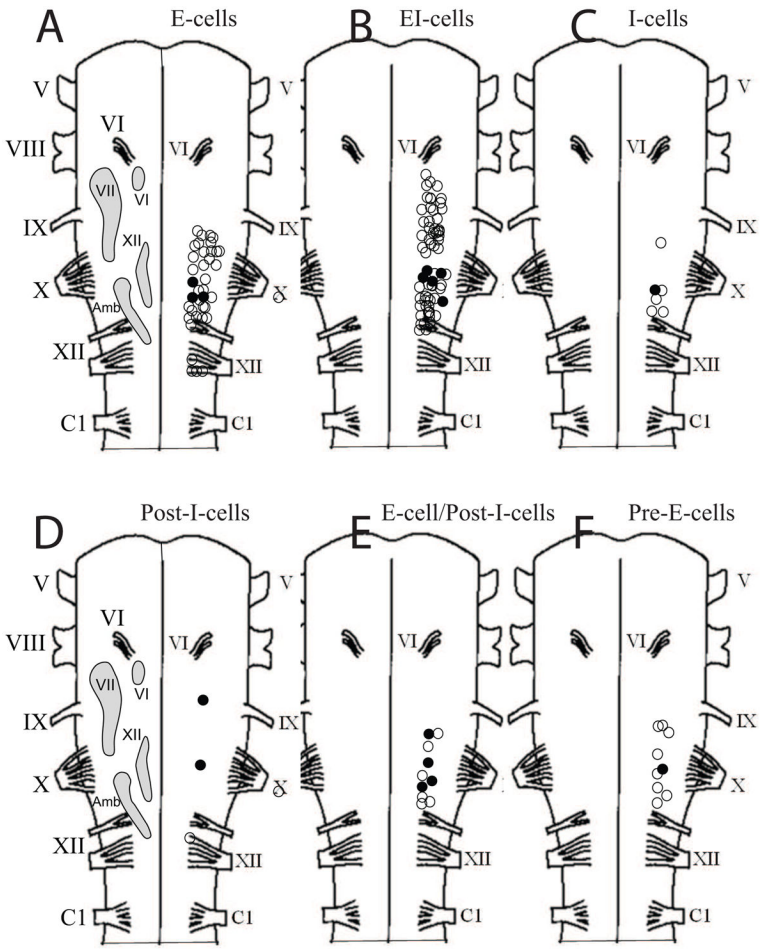

Fig. 3.

Diagrams of turtle hemibrainstems with approximate locations of specific nuclei (labeled light gray shapes) included for reference, such as the abducens nucleus (VI), facial nucleus (VII), hypoglossal nucleus (XII), and *nucleus ambiguus* (Amb), which were modified from Cruce and Nieuwenhuys (1974). The location of most neurons within each class is shown. The position of the neurons were not located with respect to depth and mediolateral location. Open circles indicate neuron location, while filled circles indicate that the neuron had intrinsic bursting properties.

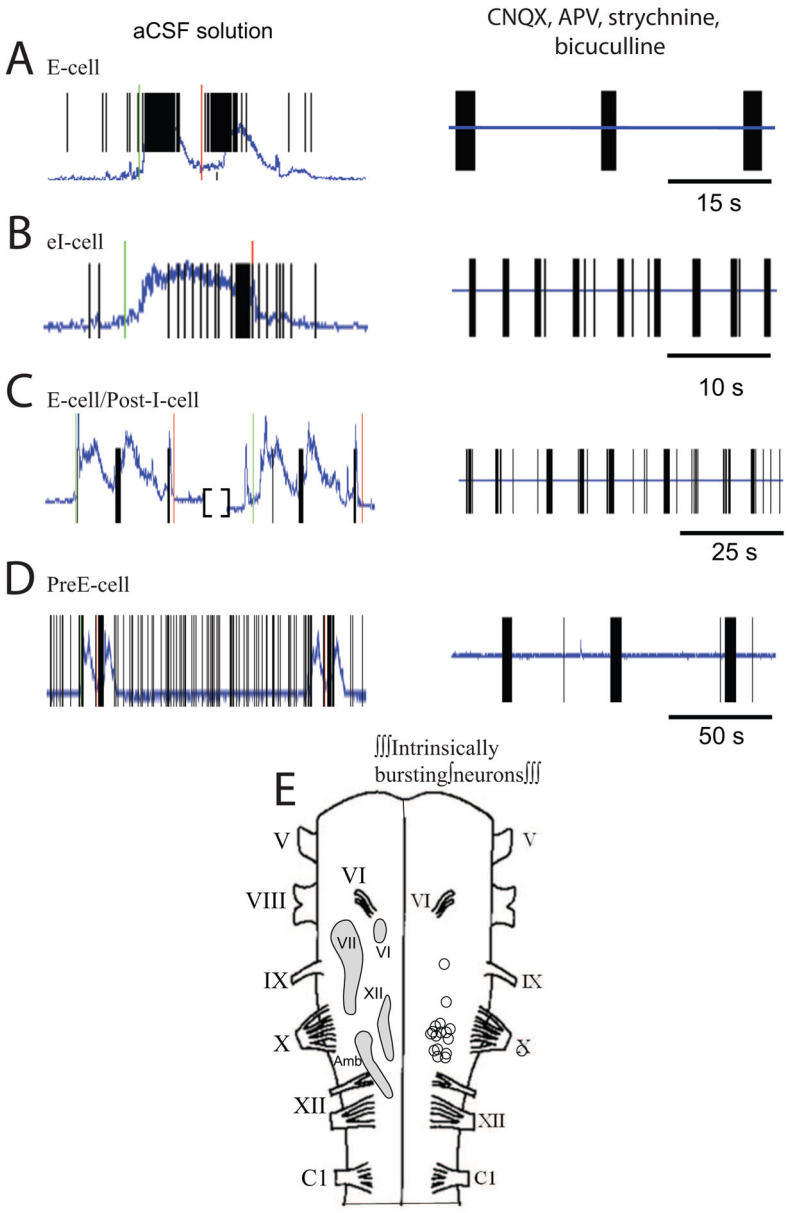

Fig. 4.

Examples of respiratory neurons in aCSF solution (left panels) that have intrinsic bursting properties when bathed in synaptic blockade solution containing CNQX, APV, strychnine, and bicuculline with (right panels). The intrinsically bursting respiratory neurons include an E-cell (A), EI-cell (B), E-cell/Post-I-cell (C), and a Pre-E-cell (D). The integrated respiratory motor output recorded on XII nerve root is shown as a blue trace and the timing of action potential firing is indicated by the vertical lines. (E) Diagrams of turtle hemibrainstem with the rostrocaudal location of all intrinsically bursting respiratory neurons shown (open circles).

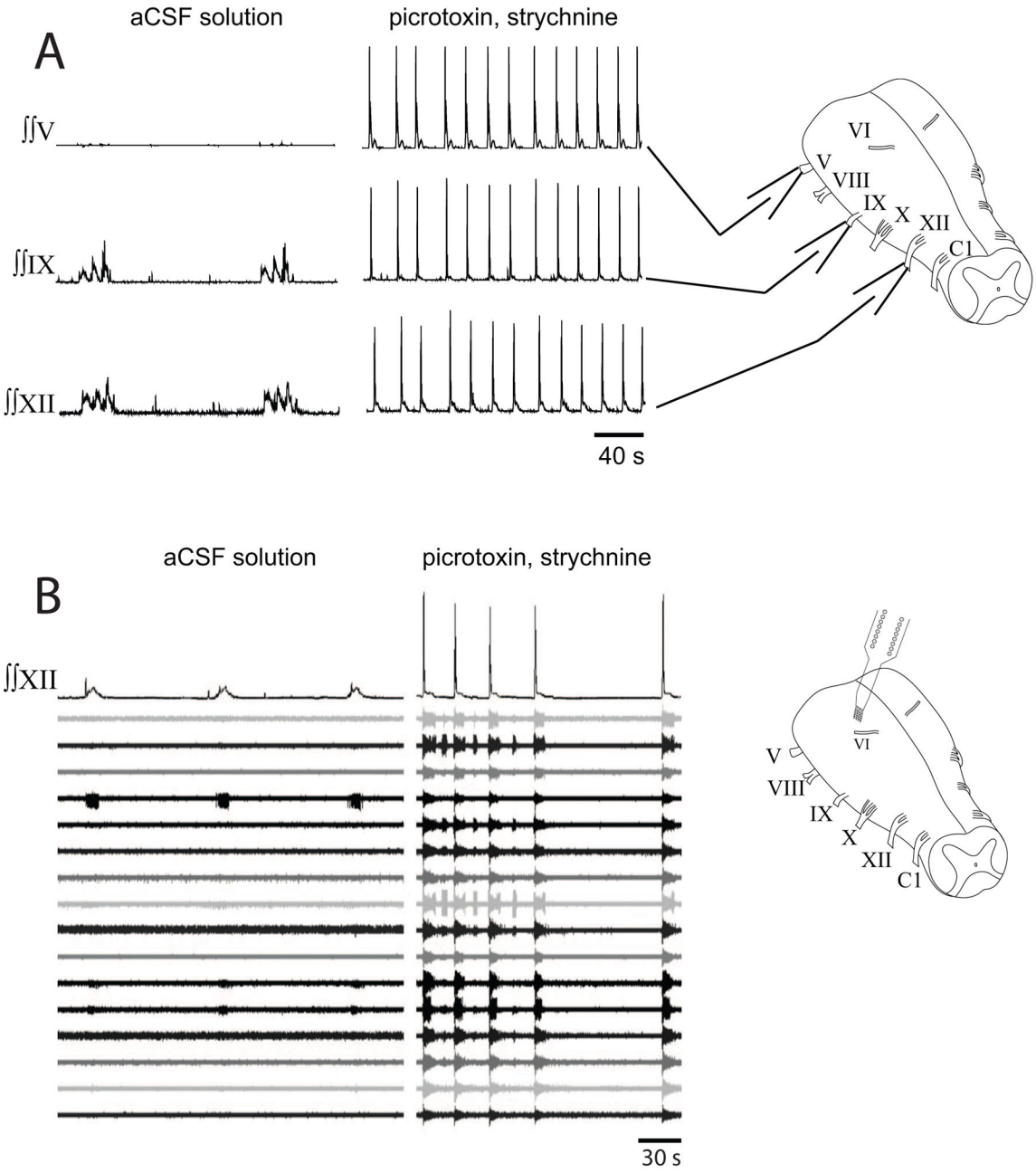

Fig. 5.

Seizure activity in turtle brainstem induced by synaptic inhibition blockade. (A) Recordings of integrated motor output on roots of cranial nerves V, IX, and XII under control conditions (aCSF solution; left panels), and during synaptic inhibition blockade (picrotoxin, strychnine; right panels). Rhythmic activity on IX and XII roots was transformed into large synchronous bursts on all roots. (B) Recordings of integrated XII motor output along with 16 extracellular recordings from a pontine site rostral to cranial nerve root VI (see diagram at right) under control conditions (left panel) and during synaptic inhibition blockade (right panel).

Synchronized bursts of action potentials were observed on all channels during synaptic inhibition blockade.

Table 1

Respiratory neuron classification (classification in parentheses corresponds to scheme in Takeda et al., 1986), activity pattern, number of neurons, peak firing rate (mean ± standard deviation, range) derived from cycle-triggered histograms, and the number of intrinsically bursting neurons are shown (number of intrinsically bursting neurons/total number tested in that group).

Neuron classification	Activity pattern	Neurons (n)	Peak rate (Hz)	Intrinsically bursting neurons
E-cell (E)	peak activity and most activity during first two-thirds of XII burst	50	10.5 ± 9.5 (0.1–37.0)	3/38
EI-cell (E-i)	active throughout entire XII burst	133	15.1 ± 12.5 (0.8–53.0)	5/118
I-cell (I)	most activity during last third of XII burst	6	5.0 ± 3.7 (1.1–10.0)	1/6
Post-I-cell (PI)	peak activity at end of XII burst	3	2.5 ± 2.0 (1.2–4.8)	2/2
E-cell/Post-I- cell (pi-E)	similar to Post-I-cell, but with some activity during prior to or during first two-thirds of XII burst	11	6.8 ± 3.4 (1.6–12.0)	4/7
Pre-E-cell	peak activity prior to or at onset of XII burst	9	15.8 ± 12.7 (1.7–42.0)	1/6
Respiratory- related unit	peak activity during XII burst, but can’t be classified	7	2.3 ± 2.5 (0.4–7.1)	3/5